processes

MDPI

Article

Kinetic Analysis of Pyrolysis Reaction of Hydrogen-Containing Low Rank Coals Based on Thermogravimetric Method

Qiyuan Mi [1], Bin Li [1], Yifan Li [2], Yue Ma [3] and Ruimeng Shi [1,*,†]

[1] School of Metallurgical Engineering, Xi'an University of Architecture and Technology, Xi'an 710055, China
[2] Huatian Engineering & Technology Corporation, MCC, Nanjing 210019, China
[3] NCS Testing Technology Co., Ltd., Beijing 100081, China
* Correspondence: shiruimeng@163.com; Tel.: +86-18009185550
† Graduated from Chongqing University and earned a doctorate. Now he works at Xi'an University of Architecture and Technology as a master tutor.

Abstract: Based on the combined technology of thermogravimetric analysis-mass spectrometry (TG-MS), the non isothermal kinetic of two low rank coals with high hydrogen content and the release characteristics of H_2 in volatiles were explored. The effect of coal species and coal particle size on pyrolysis was studied. The CR (Coats-Redfern) method and the DAEM (Distributed activation energy model) method were used to construct the pyrolysis kinetic model by dividing temperature stages, and the results showed that the mechanisms of pyrolysis process of lower rank coals were mainly 3-D diffusion (G-B) and Growth of nucleation (Avrami-Erofeev, n = 1/3). The use of the DAEM method made up for the shortcomings of the CR method in calculating the activation energy, and the analysis of coal pyrolysis kinetics was more comprehensive. The higher the volatile content the coal contained, the lower activation energy the pyrolysis process would require. The larger the particle size of the coal was, the higher activation energy the pyrolysis process would need. The release law of H_2 in low rank coal during the pyrolysis process was analyzed by mass spectrometry, and results were presented: the first peak occurs at 500 °C and the second at 750 °C, which was mainly generated by the condensation and dehydrogenation reactions of aromatic compounds.

Keywords: low rank coal; volatiles; pyrolysis kinetics; DAEM model

Citation: Mi, Q.; Li, B.; Li, Y.; Ma, Y.; Shi, R. Kinetic Analysis of Pyrolysis Reaction of Hydrogen-Containing Low Rank Coals Based on Thermogravimetric Method. *Processes* **2023**, *11*, 706. https://doi.org/10.3390/pr11030706

Academic Editor: Song Hu

Received: 17 January 2023
Revised: 7 February 2023
Accepted: 23 February 2023
Published: 27 February 2023

1. Introduction

At present, the vast majority of iron is produced by using coke to reduce iron ore in the blast furnace [1]. Coke reduces iron oxides to metallic iron at high temperatures such that large amounts of CO and CO_2 are released [2]. However, with the increasing shortage of coking coal resources and the increasingly strict environmental protection requirements, the steel industry urgently needs to explore an iron-making process that can use non-coking coal and is environmentally friendly [3]. Based on the above requirements, direct reduction ironmaking process was developed by researchers [4]. Due to the relative lack of natural gas resources, the development of gas based reduction in China is restricted [5]. However, China has a large number of coal reserves, especially the low rank coal which is characterized by high volatile content, high chemical activity, and high economic value [6]. It is an ideal raw material for the development of coal-based direct reduction. Based on the above characteristics, China has the potential to develop a coal-based direct reduction iron-making process.

The pyrolysis process of low rank coal is the initial reaction of reductant source in the coal-based reduction process, and the volatiles of the gas pyrolysis product such as H_2 has a significant effect on the subsequent reduction process of iron oxides, which is an ideal reductant for reduction of iron ore. Previous research by our research group has proved that the volatiles released by the pyrolysis of coal participate in the reduction of iron oxides and accelerate the process of the reduction reaction [7]. The pyrolysis process

of coal is a very complex reaction, especially for low rank coals with high volatile content. There is a certain degree of difference in the volatile content for different low rank coals. Therefore, during the pyrolysis process, the influence of these differences on the pyrolysis characteristics and kinetic mechanism of pyrolysis of coal is still not clear.

For the factors affecting the pyrolysis of coal, there have been a large number of studies in the past, and the main influencing factors include the type of coal, heating rate, the particle size of coal, end temperature of pyrolysis, the atmosphere of pyrolysis, etc. Xie [8] studied the influence of the end temperature of pyrolysis and heating rate on the pyrolysis of different low rank coals, and the results showed that: the more volatile content the low rank coal contained, the easier the pyrolysis reaction would carry out; when the temperature of pyrolysis was higher than 800 °C, an increase of temperature had few effects on the pyrolysis process of low rank coal, and the pyrolysis reaction was basically over. Zhang [9] studied the effect of heating rate on the pyrolysis characteristics of Zhundong lignite, and the results showed that: the appropriate heating rate could promote the generation and release of volatiles, help the construction of pore channels and pore size distribution, and hinder pore blockage caused by thermal polycondensation. Peng [10] explored the influence of the particle size of coal on pyrolysis characteristics, and selected lignite coal samples with four particle size range below 1 mm, and the results showed that: the larger the particle size of the coal particles was, the higher the average activation energy the pyrolysis process would need. However, there is relatively little research on the effect of volatile content in coal-on-coal pyrolysis. This paper focuses on the influence of volatile content in coal on the pyrolysis process of coal.

Regarding the kinetics of pyrolysis of coal, non-isothermal methods are still commonly used. The current main methods include the Kissinger-Akah-Sunose (KAS) method, the Flynn-Ozawa-Wall (FOW) method, the DAEM (Distributed activation energy model) method, the Coats-Redfern (CR) method [11]. DAEM method treats complex pyrolysis reactions as consisting of many independent parallel elementary reactions; the DAEM method can continuously present the distribution of the activation energy of the fracture and generation of various chemical bonds in the pyrolysis process, and the obtained activation energy value becomes a function of change with the extent of conversion, which is helpful for the specific study of each stage of pyrolysis [12]. The CR method regards the whole pyrolysis process under a single heating rate as a research object. The advantage of the CR method is that it can solve the mechanism of the pyrolysis process, but the disadvantage is that the activation energy value is greatly affected by the selection of model functions and pyrolysis conditions, which may introduce a lot of error. According to the slope trend of $\ln\left[g(\alpha)/T^2\right]$ versus $1/T$, Guo [13] divided the pyrolysis process of coal into low temperature section and high temperature section, substituted different model functions, linear fitting, and selected the function with the highest fitting degree as the reaction mechanism, and the results showed that the 2-stage shrinking core model is the mechanism of the pyrolysis process. However, different researchers often obtain inconsistent conclusions [14]. This reflects a phenomenon: the mechanism of the pyrolysis process is greatly related to the type of coal, and secondly, the difference in pyrolysis conditions and kinetic calculation methods will also affect the kinetic mechanism obtained. As mentioned earlier, the CR method has a unique advantage in analyzing the mechanism of the pyrolysis process, but the activation energy obtained is a single, static value, which can only make macroscopic judgments for each stage of pyrolysis process, and cannot analyze the specific process of pyrolysis. Therefore, on the basis of applying the CR method to analyze the kinetic mechanism of pyrolysis process, this paper combines the DAEM method to analyze the activation energy value of the pyrolysis process of coal with each extent of conversion which is a "dynamic" value, and the real-time change of pyrolysis reaction can be analyzed from the microscopic level.

There are many factors affecting the pyrolysis process of coal, and this paper focuses on the influence of volatile content in coal on the pyrolysis process of coal. In this paper, two low rank coals with different volatile content were selected to calculate the characteristic parameters and activation energy of the pyrolysis process. In order to further illustrate the effect of volatile content on the pyrolysis process of coal, a low rank coal and coke were selected for uniform mixing in different proportions, and their pyrolysis characteristic parameters and pyrolysis activation energy were calculated. At the same time, the release characteristics of H_2 in the volatile components were analyzed by a mass spectrometer. The objectives of the work in this paper are to study the release mechanism of volatiles in the pyrolysis process of coal and the influence of volatile content on the pyrolysis process of coal, explore the kinetic mechanism of controlling the pyrolysis process of low rank coal and lay the groundwork for the study of coal-based direct reduction with low rank coal as reductant.

2. Experimental

2.1. Materials

The characteristics of coal are diverse and complex. According to the degree of coalification from high to low, it can be roughly divided into anthracite, bituminous coal, and lignite; lignite is the main component of low rank coal. The experimental samples were two kinds of low rank coal in Xinjiang and northern Shaanxi, China, and were named 1# and 2# respectively; a type of coke was chosen. The proximate analysis of coal is performed based on GB/T 212-2008 and the results of the proximate analysis are shown in Table 1.

Table 1. The proximate analysis of coal (mass%).

	A_{ad}	M_{ad}	FC_{ad}	V_{ad}
1#	5.49	5.91	43.26	45.34
2#	5.76	6.88	52.29	35.07
coke	12.46	0.49	86.55	0.50

M—Moisture; A—Ash; V—Volatile; FC—Fixed carbon; ad—air dried basis.

2.2. Experimental Method

The pyrolysis experiments were performed in a TG-MS device (TG, SETARAM, SETSYS Evolution, France; MS, Vacuum OmniStar, Pfeiffer, Berlin, Germany). A schematic diagram of the device was shown in Figure 1. The main part of the device was made up of an automatic balance, sensors, a corundum crucible, and thermocouples. Before the beginning of the experiment, a 10.0 mg sample was weighed and placed into a crucible. The crucible was placed on a tray that connected to the sensor which effectively recorded the mass change of the sample. The real-time temperature was recorded by thermocouples. The signal of real-time temperature and mass change was received by the computer. During the experiment, Ar was used as the carrier gas at a flow rate of 50 mL/min, while Ar also served as the protective gas of the thermogravimetric balance. In this study, the sample was heated from 50 to 1000 °C at three different heating rates (10, 20, and 30 °C/min).

2.3. Kinetic Analysis

2.3.1. Pyrolysis Characteristic Parameters of Coal

The pyrolysis characteristic parameters are the most intuitive characterization of the activity of the pyrolysis reaction of the coal [15]. At present, there are two common pyrolysis characteristic parameters of coal, namely: the characteristic parameter of volatile emissions D and the characteristic index of pyrolysis P, their expressions are shown below [10].

$$D = \left[\frac{(dW/dT)_{max}}{T_{max} \times T_s \times \Delta T_{1/2}} \right] \quad (1)$$

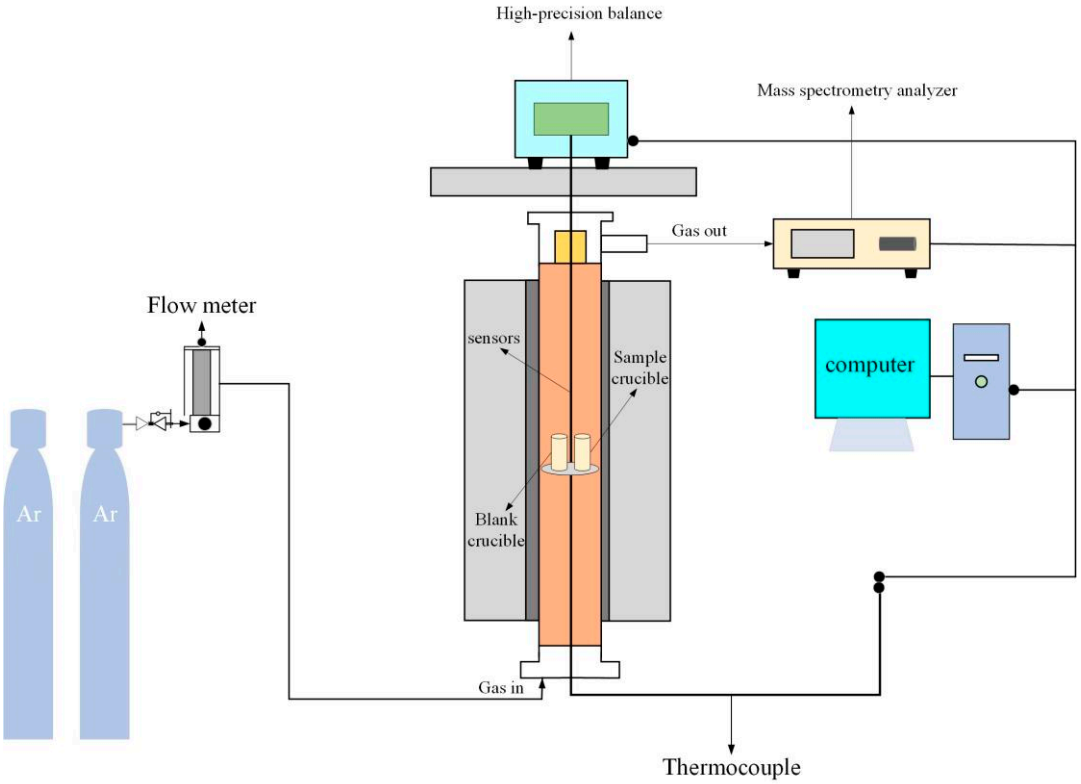

Figure 1. The schematic diagram of thermogravimetric analysis-mass spectrometry device.

Among them, the larger the D value is, the better the release characteristics of volatiles during the pyrolysis of coal will be, and the easier the pyrolysis reaction is to carry out. The initial release temperature T_s of volatiles is an important indicator to measure the difficulty of the release process of volatiles, and the temperature is determined by the tangential lines method. The maximum release rate of volatiles $(dW/dT)_{max}$ is an important indicator to measure the intensity of the release of volatiles in the pyrolysis process. The temperature corresponding to the maximum release rate of volatiles T_{max} represents the average stability of the macromolecular structure in the coal. The half-peak width $\Delta T_{1/2}$ is the temperature interval corresponding to $(dW/dT)/(dW/dT)_{max} = 1/2$, which represents the concentration of the release of products from the pyrolysis process of coal, and the lower the value is, the more concentrated the release of volatiles will be.

In order to analyze the pyrolysis process more comprehensively, the characteristic index of pyrolysis P is introduced, which can reflect the pyrolysis reaction activity of coal in the entire pyrolysis interval [13].

$$P = \left[\frac{(dW/dT)_{max} \times (dW/dT)_{mean} \times \Delta W_{max}}{T_0 \times (T_f - T_0)} \right] \quad (2)$$

In this paper, the temperature corresponding to the extent of conversion α reaches 10% is defined as the initial pyrolysis temperature T_0. The temperature corresponding to the extent of conversion α reaches 90% is defined as the final pyrolysis temperature T_f. $(T_f - T_0)$ is the temperature range of the pyrolysis process. $(dW/dT)_{max}$ is the maximum weight loss rate during pyrolysis process. $(dW/dT)_{mean}$ is average weight loss rate during the pyrolysis process. ΔW_{max} is maximum weight loss during the pyrolysis process.

The pyrolysis of coal is a very complex heterogeneous reaction, so it is difficult to define the precise initial temperature and end temperature of the pyrolysis reaction of coal by physical and chemical detection means. Moreover, the pyrolysis process of coal generally carries out in three stages. The release of volatile gases focused on in this paper is mainly in the second stage and third stages of the pyrolysis process of coal, and the corresponding conversion rate is basically in the range of 10–90%. Therefore, in order to facilitate the calculation of the characteristic parameters of pyrolysis of coal, this paper uniformly defines the initial temperature of pyrolysis of coal as the corresponding temperature when the conversion rate reaches 10%; the end temperature of pyrolysis of coal is defined as the corresponding temperature when the conversion rate reaches 90%.

2.3.2. Pyrolysis Kinetic Model

Classical metallurgical kinetic models are based on isothermal reactions and homogeneous reactions, and the resulting kinetic parameter, such as activation energy, is also known as apparent activation energy [16]. The pyrolysis of coal is a very complex heterogeneous reaction process, which also carries out in a temperature range [17]. Then, according to the idea of the microelement method, the process of non-isothermal reaction is decomposed into infinitesimal time intervals, then each time interval can be regarded as an isothermal process; similarly, the pyrolysis reaction of coal can also be regarded as consisting of multiple homogeneous reactions [14]. Moreover, the pyrolysis reaction of coal carries out in several stages. The temperature range of the first stage is from room temperature to 300 °C, which manifests itself as dry degassing of coal. The second stage is mainly based on the depolymerization and decomposition reaction of coal accompanied by a large number of volatiles released; the temperature range at this stage is 300–600 °C. The third stage is the stage of semi-coke condensation into char; the temperature range at this stage is 600–1000 °C. The amount of tar precipitated at this stage is very small, and the volatiles released are mainly hydrocarbon gases, H_2, and carbon oxides [10].

In this paper, the activation energy of the pyrolysis process is calculated in several stages, in order to approximate and compare the difficulty of the reaction of coal at different stages from the side, and then explore the pyrolysis mechanism of coal.

The establishment of the pyrolysis kinetic model is first to determine the extent of conversion α.

$$\alpha = \frac{W_0 - W}{W_0 - W_\infty} \tag{3}$$

where W is the instantaneous mass of the sample and parameters W_0 and W_∞ are the initial and final mass of the sample, respectively. In this study, $(W_0 - W)$ is the actual mass loss, and $(W_0 - W_\infty)$ is considered as the theoretical maximum mass loss. The reaction rate is shown in Formula (4) [18].

$$\frac{d\alpha}{dt} = A \times \mathrm{f}(\alpha) \times e^{-\frac{E}{\mathrm{RT}}} = \beta \frac{d\alpha}{dT} \tag{4}$$

where A is the pre-exponential factor, E is the activation energy, $\mathrm{f}(\alpha)$ is the differential conversion function, and R is the gas constant. The integral form of the mechanism function $\mathrm{g}(\alpha)$ is shown in Formula (5) [19].

$$\mathrm{g}(\alpha) = \int_0^\alpha \frac{d\alpha}{\mathrm{f}(\alpha)} = \frac{A}{\beta} \int_{T_0}^{T} e^{-\frac{E}{\mathrm{RT}}} dT \tag{5}$$

Combining Formulas (3)–(5) can derive Formula (6).

$$\frac{\mathrm{g}(\alpha)}{T^2} = \frac{A\mathrm{R}}{\beta E} \times \left(1 - \frac{2\mathrm{R}T}{E}\right) \times e^{-\frac{E}{\mathrm{RT}}} \tag{6}$$

Take the logarithm of Formula (6) to get Formula (7) which is the expression of the Coats-Redfern method [20].

$$\ln\left[\frac{g(\alpha)}{T^2}\right] = \ln\left[\frac{AR}{\beta E}\right] - \frac{E}{RT} \tag{7}$$

This method defines the model with the best fitting degree as the kinetic mechanism of the reaction.

The method of Distributed activation energy model (DAEM) is a type of model-free isoconversional method and is often applied when calculating the activation energy of the thermal decomposition process of substances [21]; the equation is shown in Formula (8) [22]; the activation energy can be calculated from the slope of the linear regression of $\ln\left[\beta/T^2\right]$ versus $1/T$.

$$\ln\left[\frac{\beta}{T^2}\right] = \ln\left[\frac{AR}{E}\right] + 0.6075 - \frac{E}{RT} \tag{8}$$

Common reaction kinetic mechanism functions are shown in Table 2.

Table 2. Common kinetic reaction mechanism functions.

g(α)	Function	Mechanism
g(α)1	$-\ln(1-\alpha)$	Chemical reaction (n = 1)
g(α)2	$(1-\alpha)^{-1}-1$	Chemical reaction (n = 2)
g(α)3	$\left[(1-\alpha)^{-2}-1\right]/2$	Chemical reaction (n = 3)
g(α)4	$[-\ln(1-\alpha)]^{\frac{1}{2}}$	Growth of nucleation (Avrami-Erofeev, n = 2)
g(α)5	$[-\ln(1-\alpha)]^{\frac{1}{3}}$	Growth of nucleation (Avrami-Erofeev, n = 3)
g(α)6	$[-\ln(1-\alpha)]^{2}$	Growth of nucleation (Avrami-Erofeev, n = 1/2)
g(α)7	$[-\ln(1-\alpha)]^{3}$	Growth of nucleation (Avrami-Erofeev, n = 1/3)
g(α)8	$1-(1-\alpha)^{\frac{1}{2}}$	Shrinking core model (n = 2)
g(α)9	$1-(1-\alpha)^{\frac{1}{3}}$	Shrinking core model (n = 3)
g(α)10	$1-(1-\alpha)^{2}$	Shrinking core model (n = 1/2)
g(α)11	$1-(1-\alpha)^{3}$	Shrinking core model (n = 1/3)
g(α)12	α^2	1-D diffusion
g(α)13	$\alpha+(1-\alpha)\ln(1-\alpha)$	2-D diffusion
g(α)14	$1-\frac{2}{3}\alpha-(1-\alpha)^{\frac{2}{3}}$	3-D diffusion (G-B)
g(α)15	$\left[1-(1-\alpha)^{\frac{1}{3}}\right]^{2}$	3-D diffusion (Jander, n = 2)

3. Results and Discussion

3.1. Characteristics of the Pyrolysis Reaction

Figure 2 shows the thermogravimetric test results of 1#coal and 2#coal. As can be seen from Figure 2, the peak rate of pyrolysis of coal occurs at 400–500 °C. At this time, it corresponds to the second stage of the pyrolysis process: the side chains of macromolecular aliphatic hydrocarbons and aromatic hydrocarbons in the coal begin to break, generating a large amount of tar and volatiles [10]. With further increase in temperature, the organic matter in the coal undergoes polycondensation reaction to form char, the amount of tar and volatiles produced decreases, and the changes of TG and dTG curves gradually flatten.

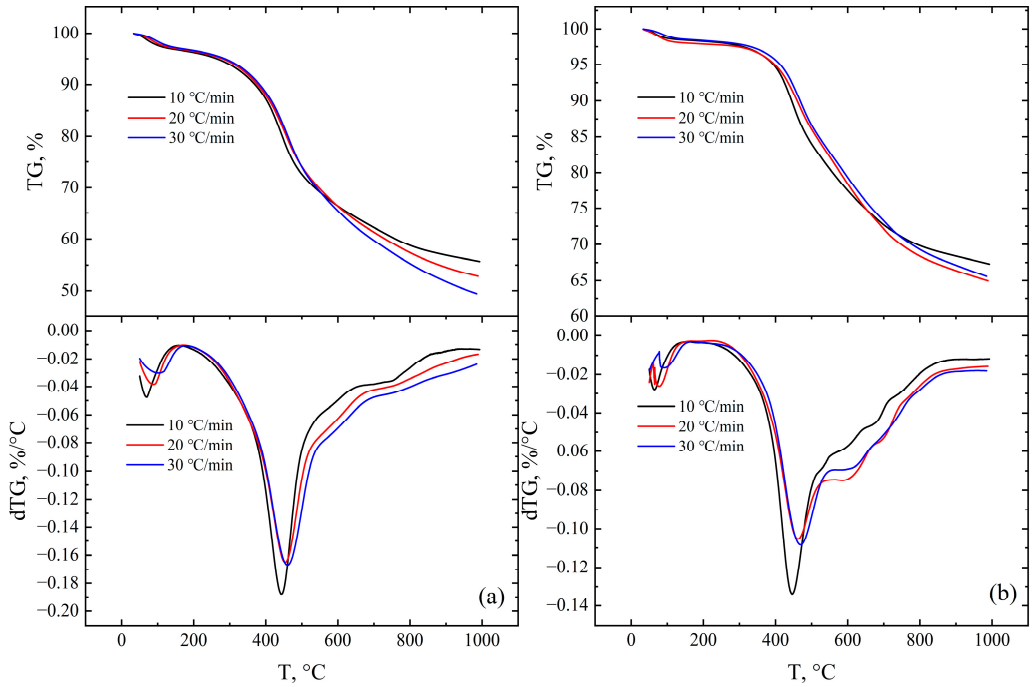

Figure 2. TG-dTG profiles for 1#coal and 2#coal. (**a**): 1#coal; (**b**): 2#coal.

3.1.1. Calculation of Pyrolysis Characteristic Parameters of Coal

According to the curves of TG-dTG of the two coals, the pyrolysis characteristic parameters of 1#coal and 2#coal are calculated. The results are shown in Tables 3 and 4.

Table 3. The characteristic parameter of volatile emissions D of 1#coal and 2#coal.

1#coal	T_s	$(dW/dT)_{max}$	T_{max}	$\Delta T_{1/2}$	|D|
10 °C/min	364 °C	−0.188%/°C	444 °C	106 °C	1.097×10^{-8}%·°C^{-3}
20 °C/min	356 °C	−0.168%/°C	456 °C	140 °C	7.392×10^{-9}%·°C^{-3}
30 °C/min	368 °C	−0.175%/°C	463 °C	145 °C	7.083×10^{-9}%·°C^{-3}
2#coal	T_s	$(dW/dT)_{max}$	T_{max}	$\Delta T_{1/2}$	|D|
10 °C/min	387 °C	−0.134%/°C	446 °C	131 °C	5.926×10^{-9}%·°C^{-3}
20 °C/min	388 °C	−0.101%/°C	461 °C	268 °C	2.107×10^{-9}%·°C^{-3}
30 °C/min	401 °C	−0.113%/°C	467 °C	271 °C	2.226×10^{-9}%·°C^{-3}

Table 4. The characteristic index of pyrolysis P of 1#coal and 2#coal.

1#coal	T_0	T_f	ΔW_{max}	$(dW/dT)_{max}$	$(dW/dT)_{mean}$	P/%^{3}·°C^{-4}
10 °C/min	240 °C	745 °C	35.46%	−0.188%/°C	−0.069%/°C	3.795×10^{-8}
20 °C/min	256 °C	792 °C	37.73 %	−0.168%/°C	−0.072%/°C	3.326×10^{-8}
30 °C/min	286 °C	819 °C	40.46%	−0.175%/°C	−0.076%/°C	3.531×10^{-8}
2#coal	T_0	T_f	ΔW_{max}	$(dW/dT)_{max}$	$(dW/dT)_{mean}$	P/%^{3}·°C^{-4}
10 °C/min	346 °C	767 °C	26.17%	−0.134%/°C	−0.065%/°C	1.565×10^{-8}
20 °C/min	361 °C	795 °C	28.04%	−0.101%/°C	−0.064%/°C	1.157×10^{-8}
30 °C/min	375 °C	807 °C	27.53%	−0.113%/°C	−0.063%/°C	1.209×10^{-8}

The heating rate increases, T_0, T_f, T_s, and T_{max} all move to a higher temperature. The pyrolysis of coal is an endothermic process, and inside the coal particles, there are differences and inhomogeneity in heat transfer, so it takes a certain amount of time to fully pyrolyze; In the same temperature range, the faster the heating rate is, the time of the pyrolysis reaction will be correspondingly shortened, and the phenomenon of "thermal hysteresis" occurs [9].

The volatile content of different low rank coals also has a significant impact on the pyrolysis reaction. Under the same heating rate, the higher the volatile content is, the greater the characteristic index of volatile emissions D and the characteristic index of pyrolysis P will become. Xie [8] came to similar conclusions in his study.

3.1.2. Effect of Particle Size of Coal on Pyrolysis

According to the research results of predecessors, the particle size of coal also has a certain impact on the pyrolysis of coal [10]. In order to explore the influence of coal particle size on pyrolysis, three dried coal samples with particle sizes (<0.15 mm, 0.15–0.25 mm, >0.88 mm) of 1#coal were selected for the experiment; the experimental results are shown in Figure 3.

These three different particle size intervals were selected. On the one hand, the condition of the laboratory is considered, especially the caliber of the crucible where the sample is placed in the thermogravimetric instrument, which is 3 mm, so particles with too large a particle size cannot be put into the crucible. On the other hand, it references the choice of particle size intervals in the literature [23].

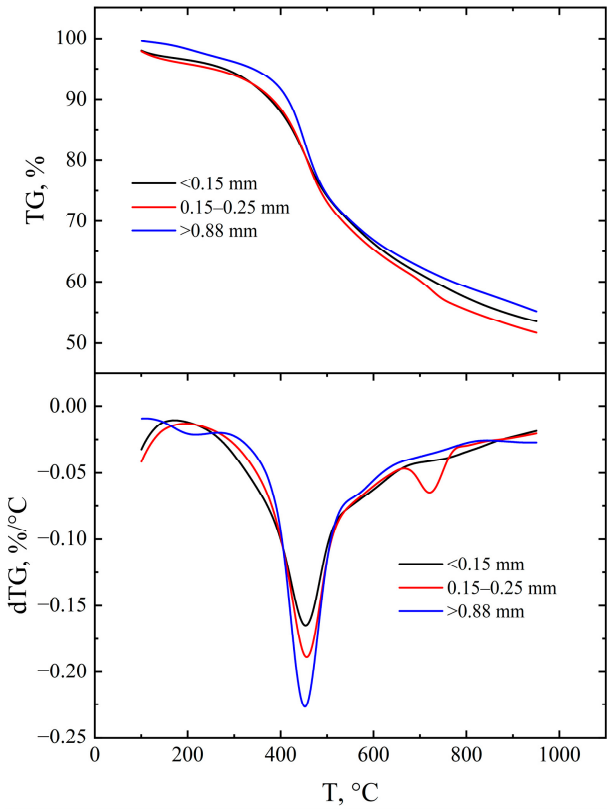

Figure 3. TG-dTG profiles for three different particle sizes of 1#coal.

From the TG curves, there is a lot of difference in mass loss between different particle sizes, but there is no correlation with the change in particle size. The maximum value of dTG is positively correlated with the particle size of coal. When the particle size of coal increased from <0.15 mm to >0.88 mm, the weight loss rate of the pyrolysis reaction is increased from 0.17%/°C to 0.23%/°C. This is consistent with the effect of the particle size of coal on the maximum weight loss rate in the study of pyrolysis characteristics of low rank coal by Tian [23].

First of all, in the pyrolysis process of coal, the volatiles will undergo a secondary reaction with the new semi coke, and carbon deposition occurs, thereby reducing the release rate and yield of the volatiles. In this experiment, the smaller the particle size is, the lower the weight loss rate will be, which is mainly attributed to the formation of metaplast. The volatilesis are mainly gas, it will form more expansion between particles; with the increase of temperature, the coal particles soften and metaplast is further generated, which hinders the diffusion of volatile gases from the surface of the coal particles to the external gas phase. For coal particles with small particle size, the gap is small, so the small gap will increase the secondary reaction between the volatiles and the new semi coke, and reduce the release of volatiles to the external gas phase. On the contrary, the gap between large particles is larger, and there will be a tendency to break violently during the heating pyrolysis process, making it easier for volatiles to diffuse to the external gas phase [23]. Therefore, coal with larger particle sizes shows a faster rate of weight loss during the pyrolysis process. However, this does not mean that the pyrolysis process of large particles of coal samples must be easy. Next, according to the TG curves, the values of activation energy of 1#coal samples with the above three different particle sizes are calculated.

The mechanism functions of Table 2 are substituted into Formula (7) for linear fitting, and the mechanism function with the highest fitting degree is selected for calculation; the results are shown in Table 5. By comparing the pyrolysis kinetic parameters of 1#coal samples with three different particle sizes, the average activation energy of the pyrolysis process of large particles is higher than that of coal particles with small particle sizes. This also reflects the fact that as the size of coal particles increases, the resistance of heat transfer also increases; the heat distribution inside coal with large particle size is uneven, the heat conduction rate is slow, and the activation energy also increases.

Table 5. Pyrolysis activation energy of 1#coal with different particle sizes.

	T, °C	E, kJ/mol	R^2	E_{mean}, kJ/mol
<0.15 mm	290–489 490–875	89.84 62.51	0.973 0.993	76.18
0.15–0.25 mm	298–484 485–896	90.15 65.95	0.948 0.988	78.05
>0.88 mm	305–479 480–926	117.72 60.05	0.932 0.984	88.89

3.2. Acquisition of the Kinetic Parameters

According to Formula (3), the extent of conversion of 1#coal and 2#coal throughout the pyrolysis process are calculated. At each heating rate β, extents of conversion are selected from 0.10 to 0.90 with an increment of 0.10 and used to calculate the activation energy of 1#coal and 2#coal using Formula (8) according to DAEM method. The values of E at each extent of conversion are presented in Figures 4 and 5.

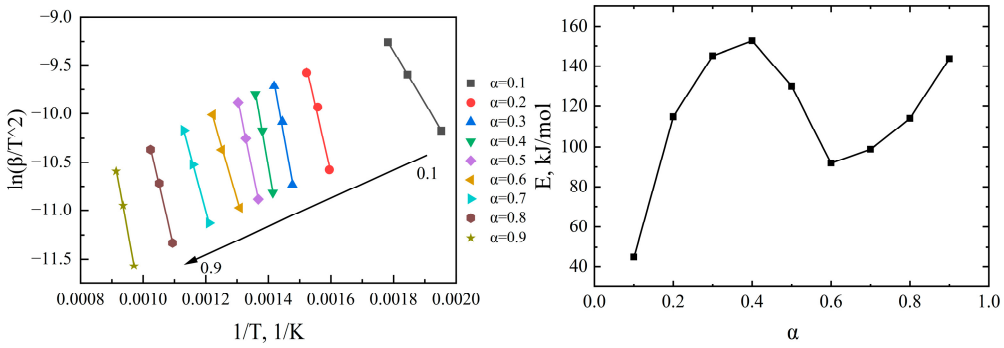

Figure 4. The activation energy of 1#coal at each extent of conversion based on DAEM method.

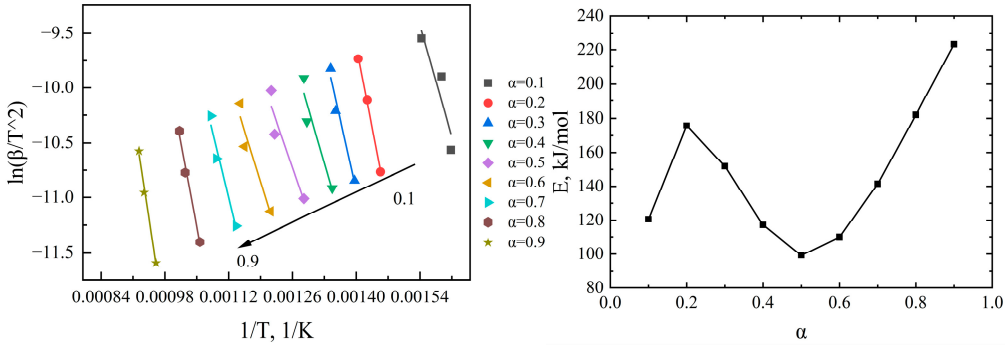

Figure 5. The activation energy of 2#coal at each extent of conversion based on DAEM method.

It is not difficult to find that the activation energy of the pyrolysis process of two kinds of low rank coal increases first, subsequently decreases, and then increases. The early activation energy increases because the corresponding stage is the second stage of the pyrolysis process, the stage where a large number of chemical bonds break, release volatiles and tar; this stage is mainly an endothermic reaction, requiring a lot of energy, so the activation energy increases. With the gradual release of volatiles and tar, the endothermic reaction weakens, and the activation energy decreases. When the temperature rises to 600 °C, the newly generated semi coke will undergo polycondensation reaction to become char. In the process of release of volatiles and tar, metaplast is also generated, which further hinders the diffusion between the gas phases, increases the diffusion resistance, and the activation energy increases again.

Combined with the above calculation results, it can be seen that the 1#coal with the higher volatile content has the lower activation energy required for the pyrolysis process, with an average value of 115.09 kJ/mol; the average activation energy of 2#coal is 146.79 kJ/mol. It can be seen that the higher the volatile content of the coal, the easier the pyrolysis reaction is to carry out, and the more fully the volatiles are released.

3.3. Analysis of the Kinetic Mechanism

The main analysis method of the kinetic mechanism of the pyrolysis process is still the CR method. There are currently two ideas for analysis of the pyrolysis kinetic mechanism by the CR method [14]. The first idea is that the pyrolysis reaction is a simple decomposition reaction, so given the mechanism function $f(\alpha) = (1-\alpha)^n$, substituted into the equation of the CR method, the following equations are shown in Formula (9):

$$\begin{aligned} \ln\left[\frac{1-(1-\alpha)^{1-n}}{T^2(1-n)}\right] &= \ln\left[\frac{AE}{\beta R}\right] - \frac{E}{RT}(n \neq 1) \\ \ln\left[\frac{-\ln(1-\alpha)}{T^2}\right] &= \ln\left[\frac{AE}{\beta R}\right] - \frac{E}{RT}(n = 1) \end{aligned} \quad (9)$$

The second idea is to substitute different model functions (Table 2) according to Formula (7), fit linear regression of $\ln\left[g(\alpha)/T^2\right]$ versus $1/T$, select the model function with the highest extent of fit as the kinetic mechanism. Due to low rank coal containing more volatiles, the pyrolysis process is complex and cannot be regarded as a simple thermal decomposition reaction; moreover, the pyrolysis process of low rank coal may be controlled by multiple models. Therefore, this paper adopts the second idea, and the fitting results of the mechanism functions of 1#coal and 2#coal are shown in Figures 6 and 7, Tables 6 and 7.

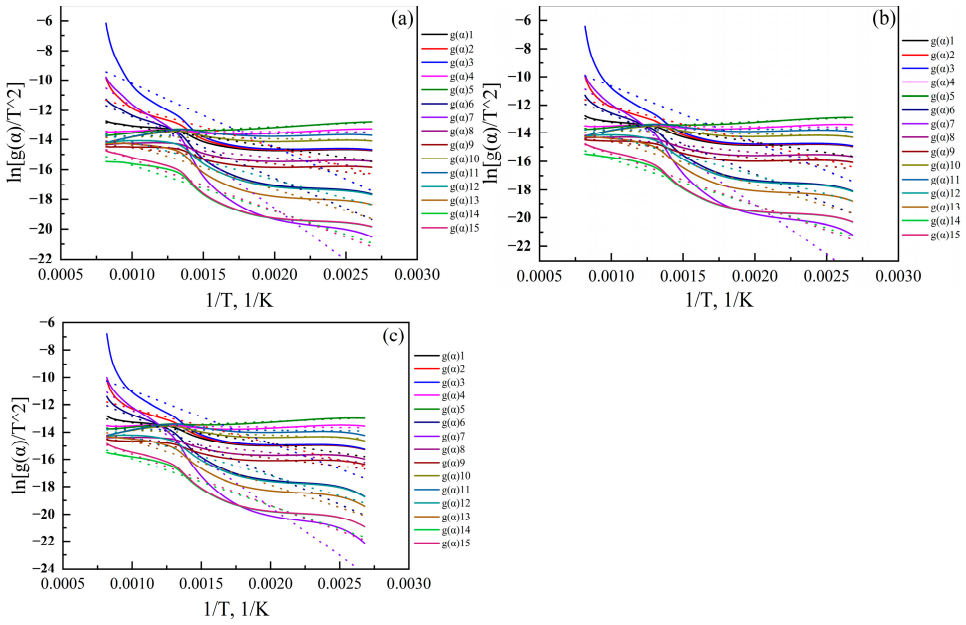

Figure 6. The fitting results of kinetic mechanism functions of 1#coal (**a**): 10 °C/min; (**b**): 20 °C/min; (**c**): 30 °C/min.

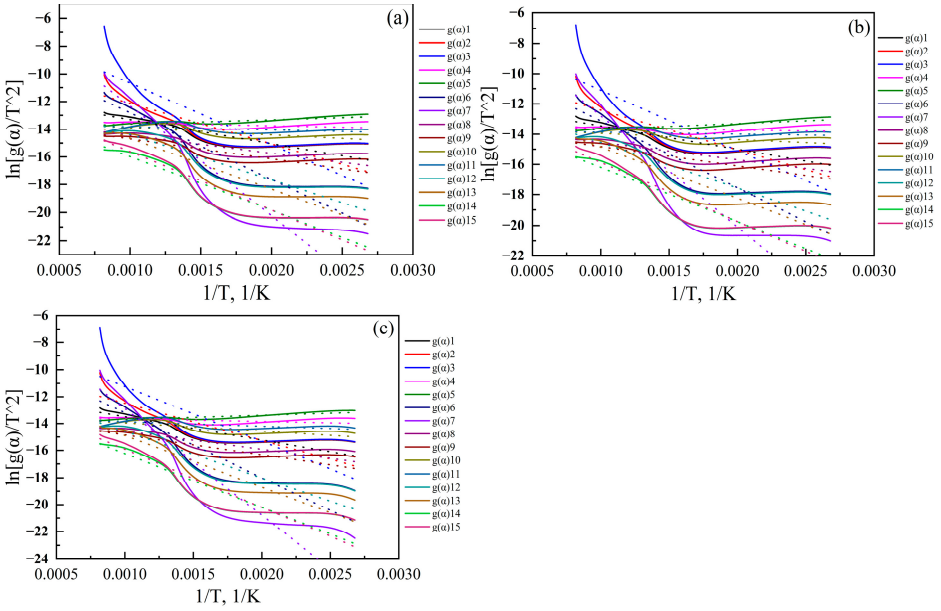

Figure 7. The fitting results of kinetic mechanism functions of 2#coal (**a**): 10 °C/min; (**b**): 20 °C/min; (**c**): 30 °C/min.

Table 6. The fitting results of kinetic mechanism functions of 1#coal.

g(α)	Function	R^2 (10 °C/min)	R^2 (20 °C/min)	R^2 (30 °C/min)
g(α)1	$-\ln(1-\alpha)$	0.883	0.887	0.894
g(α)2	$(1-\alpha)^{-1}-1$	0.825	0.819	0.828
g(α)3	$\left[(1-\alpha)^{-2}-1\right]/2$	0.762	0.750	0.757
g(α)4	$[-\ln(1-\alpha)]^{\frac{1}{2}}$	0.016	0.044	0.111
g(α)5	$[-\ln(1-\alpha)]^{\frac{1}{3}}$	0.902	0.914	0.908
g(α)6	$[-\ln(1-\alpha)]^{2}$	0.927	0.927	0.931
g(α)7	$[-\ln(1-\alpha)]^{3}$	0.935	0.935	0.938
g(α)8	$1-(1-\alpha)^{\frac{1}{2}}$	0.825	0.853	0.873
g(α)9	$1-(1-\alpha)^{\frac{1}{3}}$	0.856	0.873	0.888
g(α)10	$1-(1-\alpha)^{2}$	0.083	0.225	0.378
g(α)11	$1-(1-\alpha)^{3}$	0.094	0.008	0.018
g(α)12	α^{2}	0.901	0.915	0.926
g(α)13	$\alpha+(1-\alpha)\ln(1-\alpha)$	0.918	0.928	0.934
g(α)14	$1-\frac{2}{3}\alpha-(1-\alpha)^{\frac{2}{3}}$	0.924	0.931	0.936
g(α)15	$\left[1-(1-\alpha)^{\frac{1}{3}}\right]^{2}$	0.932	0.938	0.939

Table 7. The fitting results of kinetic mechanism functions of 2#coal.

g(α)	Function	R^2 (10 °C/min)	R^2 (20 °C/min)	R^2 (30 °C/min)
g(α)1	$-\ln(1-\alpha)$	0.821	0.759	0.807
g(α)2	$(1-\alpha)^{-1}-1$	0.787	0.725	0.761
g(α)3	$\left[(1-\alpha)^{-2}-1\right]/2$	0.734	0.677	0.703
g(α)4	$[-\ln(1-\alpha)]^{\frac{1}{2}}$	0.264	0.084	0.259
g(α)5	$[-\ln(1-\alpha)]^{\frac{1}{3}}$	0.714	0.799	0.731
g(α)6	$[-\ln(1-\alpha)]^{2}$	0.879	0.841	0.868
g(α)7	$[-\ln(1-\alpha)]^{3}$	0.892	0.859	0.881
g(α)8	$1-(1-\alpha)^{\frac{1}{2}}$	0.789	0.734	0.796
g(α)9	$1-(1-\alpha)^{\frac{1}{3}}$	0.804	0.747	0.803
g(α)10	$1-(1-\alpha)^{2}$	0.455	0.384	0.571
g(α)11	$1-(1-\alpha)^{3}$	0.149	0.063	0.305
g(α)12	α^{2}	0.867	0.843	0.874
g(α)13	$\alpha+(1-\alpha)\ln(1-\alpha)$	0.876	0.848	0.877
g(α)14	$1-\frac{2}{3}\alpha-(1-\alpha)^{\frac{2}{3}}$	0.879	0.849	0.878
g(α)15	$\left[1-(1-\alpha)^{\frac{1}{3}}\right]^{2}$	0.882	0.848	0.876

Among them, g(α)1–g(α)3 belong to the Chemical reaction model. g(α)4–g(α)7 belong to the Avrami–Erofeev model (nucleation and nuclear growth model). g(α)8–g(α)11 belong to the Shrinking core model, or interfacial reaction model. g(α)12–g(α)15 belong to the Diffusion model.

From the calculation results in Tables 6 and 7, it can be seen that the functions $[-\ln(1-\alpha)]^3$ and $\left[1-(1-\alpha)^{\frac{1}{3}}\right]^2$ have higher fitting degrees at three different heating rates, representing the mechanisms of Growth of nucleation (Avrami-Erofeev, n = 1/3) and 3-D diffusion (Jander, n = 2).

As mentioned in Section 2.3.2, the pyrolysis process of coal carries out in several stages, so the difficulty of each stage of the reaction will also be different, which is reflected in the difference in activation energy [24]. Next, the activation energy of each stage during the pyrolysis process is calculated according to the slope of $\ln\left[g(\alpha)7/T^2\right]$ versus $1/T$ and $\ln\left[g(\alpha)15/T^2\right]$ versus $1/T$ curves, the results are shown in Tables 8 and 9.

Table 8. The calculation results of activation energy at different temperature stage of 1#coal and 2#coal by g(α)7.

	β	T, °C	E, kJ/mol	R^2
1#coal	10 °C/min	220–485	69.463	0.929
	10 °C/min	486–950	58.979	0.987
	20 °C/min	283–488	87.563	0.971
	20 °C/min	489–950	63.876	0.984
	30 °C/min	296–553	96.982	0.985
	30 °C/min	554–950	67.260	0.973
2#coal	10 °C/min	296–478	113.635	0.942
	10 °C/min	479–950	76.114	0.991
	20 °C/min	310–492	101.705	0.956
	20 °C/min	493–950	88.427	0.999
	30 °C/min	326–499	122.249	0.966
	30 °C/min	500–950	88.253	0.998

Table 9. The calculation results of activation energy at different temperature stage of 1#coal and 2#coal by g(α)15.

	β	T, °C	E, kJ/mol	R^2
1#coal	10 °C/min	282–502	49.626	0.953
	10 °C/min	503–950	18.648	0.998
	20 °C/min	286–514	53.068	0.976
	20 °C/min	514–950	22.081	0.995
	30 °C/min	291–521	55.238	0.976
	30 °C/min	521–950	23.453	0.992
2#coal	10 °C/min	288–503	69.895	0.950
	10 °C/min	504–950	28.159	0.980
	20 °C/min	320–505	68.598	0.973
	20 °C/min	506–950	36.174	0.979
	30 °C/min	325–520	76.630	0.972
	30 °C/min	521–950	35.991	0.987

From the calculation results of Tables 8 and 9, the fitting degree of each stage is basically 0.95 and above, indicating that the division of temperature stages is reasonable. The lower temperature stage roughly corresponds to the second stage of pyrolysis of coal, and the higher temperature stage roughly corresponds to the third stage of pyrolysis of coal. At the same stage of the same heating rate, the activation energy of 1#coal is also lower than that of 2#coal, indicating that the more volatile content of low rank coal contains, the lower the activation energy the pyrolysis process requires, and the easier the pyrolysis is to carry out, which is consistent with the conclusion reached by Section 3.2 using the DAEM method. Under the same heating rate of the same coal species, the activation energy of the lower temperature stage is also higher than that of the higher temperature stage, indicating that there will be more chemical bond breaks in the release of pyrolysis gas and the precipitation of a large amount of tar, so a large amount of activation energy is required.

3.4. The Relationship between Volatile Content and Pyrolysis Activity

In order to further explore the relationship between volatile content and activation energy in the pyrolysis process, 1#coal and coke powders are selected and evenly mixed according to different proportions to perform thermogravimetric experiments. The coke powder has no volatiles, which acts as a control group, so several groups of samples with different proportions form a gradient on the volatile content, which is convenient for observing the law and subsequent calculation. The TG curves are shown in Figure 8.

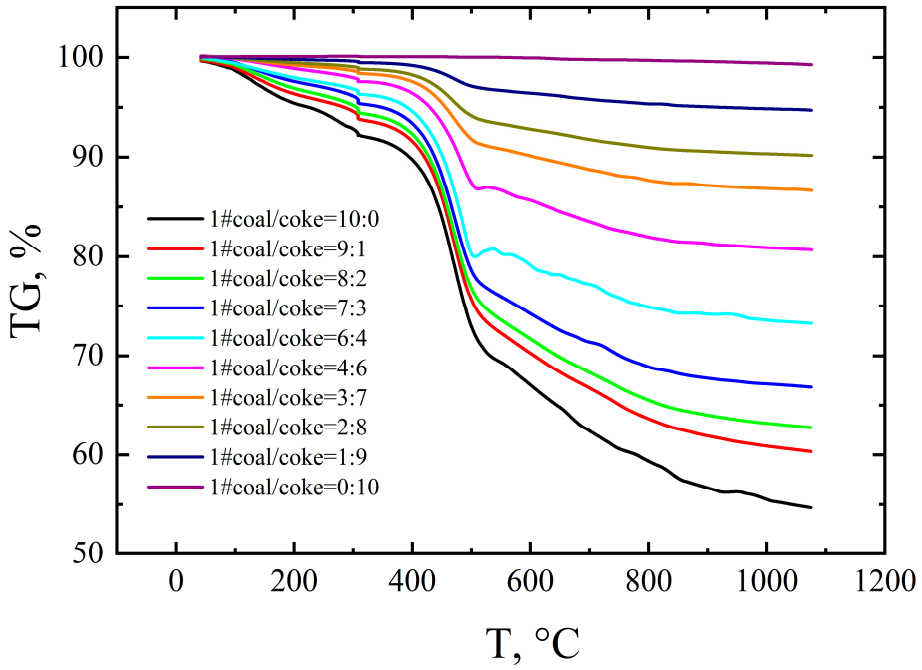

Figure 8. The TG curves of mixed powders according to different proportions from 1#coal and coke.

According to the curves of TG of the mixed powders according to different proportions from 1#coal and coke, the pyrolysis characteristic parameters are calculated. The results are shown in Table 10.

Table 10. The characteristic index of pyrolysis P of different proportions from 1#coal and coke.

1#coal/coke	T_0	T_f	ΔW_{max}	$(dW/dT)_{max}$	$(dW/dT)_{mean}$	$P/\%^3 \cdot °C^{-4}$
10:0	197 °C	805 °C	45.31%	−0.2747%/°C	−0.05865%/°C	6.09484×10^{-8}
9:1	221 °C	773 °C	39.65%	−0.2566%/°C	−0.04845%/°C	4.04075×10^{-8}
8:2	246 °C	763 °C	37.28%	−0.2504%/°C	−0.05488%/°C	4.02809×10^{-8}
7:3	272 °C	746 °C	33.15%	−0.2474%/°C	−0.05074%/°C	3.22882×10^{-8}
6:4	265 °C	745 °C	26.74%	−0.2401%/°C	−0.03564%/°C	1.79888×10^{-8}
4:6	294 °C	747 °C	19.29%	−0.1562%/°C	−0.02845%/°C	6.43651×10^{-9}
3:7	300 °C	775 °C	13.33%	−0.0854%/°C	−0.01885%/°C	1.50745×10^{-9}
2:8	307 °C	776 °C	9.82%	−0.0546%/°C	−0.0164%/°C	6.11048×10^{-10}
1:9	326 °C	835 °C	5.28%	−0.0333%/°C	−0.00835%/°C	8.84768×10^{-11}
0:10	621 °C	1046 °C	0.72%	−0.0035%/°C	−0.00136%/°C	1.31339×10^{-13}

The characteristic index of pyrolysis P is used to determine the activity of pyrolysis of coal. With the increase in the proportion of coke, the characteristic index of pyrolysis P gradually decreases, and the activity of pyrolysis gradually weakens.

Next, the activation energy values of the pyrolysis process at each mixed ratio are calculated. The CR method is applied to fit the mechanism functions in Table 2, and the activation energy values are calculated by its slope from selecting the best fitting degree. The results are shown in Table 11.

Table 11. The activation energy of pyrolysis process at each mixed ratio.

1#coal/coke	E, kJ/mol
10:0	59.56
9:1	62.91
8:2	66.67
7:3	72.29
6:4	74.73
4:6	76.65
3:7	76.71
2:8	77.00
1:9	82.75
0:10	196.33

It is not difficult to find that as the proportion of 1#coal in the mixture decreases, the activation energy required for pyrolysis increases. When the mixture is completely the coke, the pyrolysis activation energy is greatly increased.

Among the volatile gases released by the pyrolysis process of coal, the focus is on H_2. Because H_2 is a very efficient and clean reductant, it can effectively promote the reduction reaction of iron ore, and the reduction product is H_2O, which has no burden on the environment. Therefore, the release law of H_2 in the pyrolysis process of coal is clearly explored, which lays a foundation for subsequent research on the effect of volatiles on coal-based reduction.

From Figure 9, during the pyrolysis process of coal, H_2 presents two peaks. The first peak occurs at 500 °C and the second at 750 °C. By consulting the literature, it can be seen that the first peak may be due to polycondensation between free radicals; the second peak is mainly because in the late stage of pyrolysis, the condensation, and dehydrogenation between the aromatic layers, that is, a small amount of aromatic ring compounds condense into more aromatic rings, accompanied by the release of H_2 [25]. By longitudinal comparison, as the proportion of 1#coal in the mixture decreases, the relative ionic intensity of H_2 during the pyrolysis process also decreases.

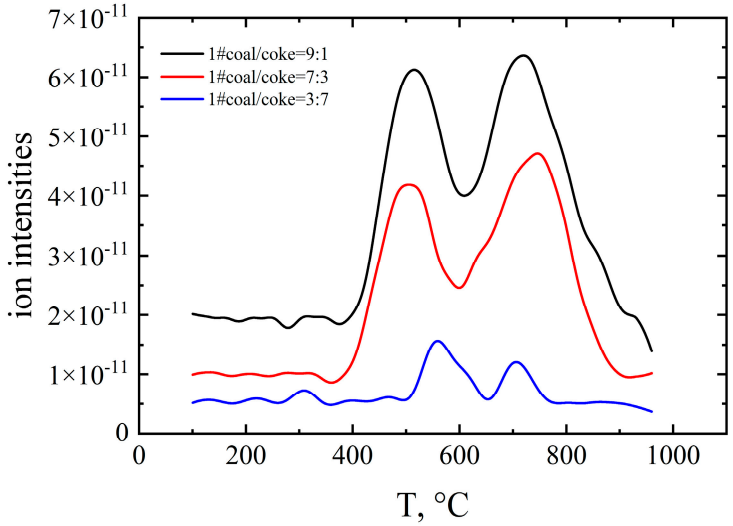

Figure 9. MS fragmented ion intensities of H_2 during the pyrolysis process of different mixed ratios.

In volatile gases, not only H_2, CH_4, and CO also have a certain reducing effect on iron ore. Therefore, the release characteristics of CH_4 and CO in the pyrolysis process are also explored. From Figure 10, during the pyrolysis process, the release of CH_4 is concentrated at 350–700 °C and the maximum peak occurs at 530 °C. The main reason for the generation of CH_4 is the cracking of bridges associated with the aliphatic side chains breakage. In addition, the reaction between carbon and hydrogen and the condensation reactions of aromatic molecules also generate CH_4 [14].

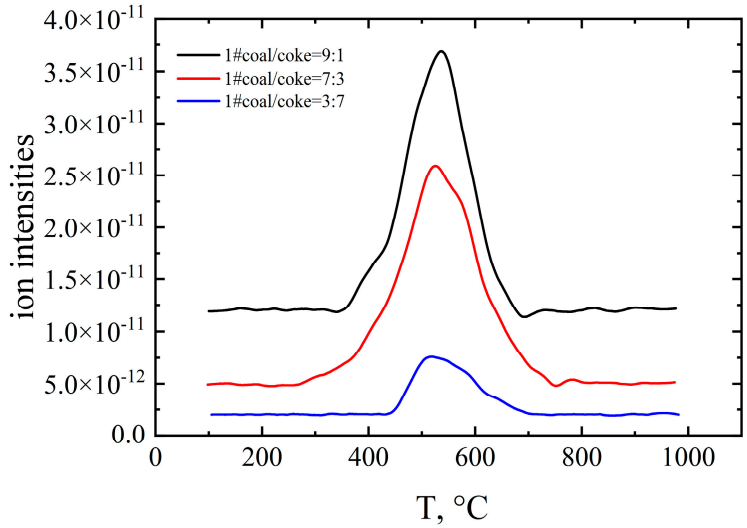

Figure 10. MS fragmented ion intensities of CH_4 during the pyrolysis process of different mixed ratios.

Figure 11 shows that CO is released in the temperature range of 420–650 °C, with a peak at 510 °C. The formation of CO is mainly due to the disintegration of weakly bonded aldehyde groups at low temperatures [17]. In some previous studies, the bond cleavage of aryl-methyl-ethers, biaryl-ethers, condensed heterocyclic oxygen-containing structures, and secondary pyrolysis reactions of tars can also generate CO [14].

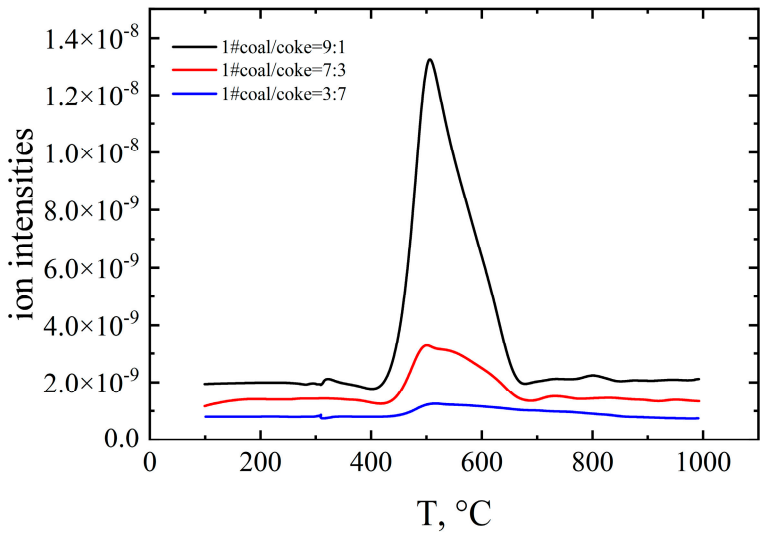

Figure 11. MS fragmented ion intensities of CO during the pyrolysis process of different mixed ratios.

4. Conclusions

Based on thermogravimetric analysis and combined with mass spectrometry analysis, the pyrolysis characteristics of coals with different volatile content are explored, and the kinetic mechanism of the pyrolysis process is analyzed. The conclusions obtained are as follows:

(1) The higher the volatile content the coal contains, the lower activation energy the pyrolysis process will need, the easier the pyrolysis reaction will carry out.
(2) The larger the particle size of coal is, the greater resistance the heat transfer will overcome; the heat distribution inside the coal with larger particles size is uneven, so the heat transfer rate is slow, and the pyrolysis activation energy also increases.
(3) The kinetic mechanisms of low rank coal in the pyrolysis process are mainly Growth of nucleation (Avrami-Erofeev, n = 1/3) and 3-D diffusion (G-B).
(4) The activation energy of the lower temperature stage of the pyrolysis process is higher than that of the higher temperature stage, indicating that there will be more chemical bond breaks in the release of volatile gas and the precipitation of a large amount of tar, so a large amount of activation energy is required.

Author Contributions: Conceptualization, Q.M. and B.L.; methodology, Q.M.; software, Q.M. and Y.L.; validation, Q.M. and B.L.; formal analysis, B.L.; investigation, Q.M.; resources, R.S.; data curation, Q.M. and Y.L.; writing-original draft preparation, Q.M.; writing-review and editing, Q.M. and B.L.; visualization, Q.M. and Y.M.; supervision, B.L. and Y.M.; project administration, R.S.; funding acquisition, R.S. All authors have read and agreed to the published version of the manuscript.

Funding: This research was funded by the China Postdoctoral Science Foundation (Grant Number 2021M702553), the Natural Science Basic Research Program of Shaanxi (Grant Number 2022JQ-428) and National Natural Science Foundation of China (Grant Number 51874224).

Data Availability Statement: Not applicable.

Conflicts of Interest: The authors declare no conflict of interest.

References

1. Sun, G.; Li, B.; Guo, H.; Yang, W.; Li, S.; Guo, J. Thermodynamic Study of Energy Consumption and Carbon Dioxide Emission in Ironmaking Process of the Reduction of Iron Oxides by Carbon. *Energies* **2021**, *14*, 1999. [CrossRef]
2. El-Geassy, A.A.; Halim, K.S.A.; Bahgat, M.; Mousa, E.A.; El-Shereafy, E.E.; El-Tawil, A.A. Carbothermic reduction of Fe_2O_3/C compacts: Comparative approach to kinetics and mechanism. *Ironmak. Steelmak.* **2013**, *40*, 534–544. [CrossRef]
3. Pineau, A.; Kanari, N.; Gaballah, I. Kinetics of reduction of iron oxides by H_2. *Thermochim. Acta* **2007**, *456*, 75–88. [CrossRef]
4. Park, H.; Sohn, I.; Freislich, M.; Sahajwalla, V. Investigation on the Reduction Behavior of Coal Composite Pellet at Temperatures between 1373 and 1573 K. *Steel Res. Int.* **2017**, *88*, 1600169. [CrossRef]
5. Wang, Y.; Li, P.; Zhu, Z. Dynamic simulation scenario analysis of multiobjective optimization configuration of China's natural gas resources. *Energy Sci. Eng.* **2020**, *8*, 3772–3787. [CrossRef]
6. Song, H.; Liu, G.; Zhang, J.; Wu, J. Pyrolysis characteristics and kinetics of low rank coals by TG-FTIR method. *Fuel Process. Technol.* **2017**, *156*, 454–460. [CrossRef]
7. Shi, R.; Li, Y.; Mi, Q.; Zou, C.; Li, B. Thermodynamic Study on the Direct Reduction of Specularite by Lignite and the Coupling Process for the Preparation of Cementitious Material. *Minerals* **2022**, *12*, 354. [CrossRef]
8. Xie, C.; Wang, Y.; Zhao, Q.; Chen, H.; Ma, H. Experimental study on Zhundong coal's pyrolysis characteristics and gasification activity. *Proc. CSEE* **2016**, *36*, 95–102.
9. Zhang, X.; Zhou, B.; An, D.; Cui, L.; Zheng, Y.; Dong, Y. Effect of heating rate on pyrolysis characteristics and char structure of Zhundong lignite coal. *J. China Coal Soc.* **2019**, *44*, 604–610.
10. Peng, Y.; Chen, S.; Sun, F.; Hu, Z.; Zhou, Y. Investigation on the kinetics of pyrolysis reaction of large coal particles based on TGA. *Clean Coal Technol.* **2021**, *27*, 128–133.
11. Lin, Y.; Li, Q.; Ji, K.; Li, X.; Yu, Y.; Zhang, H.; Song, Y.; Fu, Y.; Sun, L. Thermogravimetric analysis of pyrolysis kinetics of *Shenmu bituminous* coal. *React. Kinet. Mech. Catal.* **2014**, *113*, 269–279. [CrossRef]
12. Zhao, Y.; Qiu, P.; Xie, X.; Chen, X.; Lin, D.; Sun, S.; Liu, L. Analysis on applicability of distributed activation energy model in coal pyrolysis kinetics. *Coal Convert.* **2017**, *40*, 13–18.
13. Guo, Y.; Cheng, F. Adaptability Analysis of Kinetic Model of Blended Coal Pyrolysis. *J. Combust. Sci. Technol.* **2019**, *25*, 509–518.
14. Zou, C.; Ma, C.; Zhao, J.; Shi, R.; Li, X. Characterization and non-isothermal kinetics of *Shenmu bituminous* coal devolatilization by TG-MS. *J. Anal. Appl. Pyrolysis* **2017**, *127*, 309–320. [CrossRef]

15. Wang, J.H.; Chang, L.P. Pyrolysis Characteristics of Maceral Concentrates from Shendong Coal in Western China. *Energy Sources Part A Recovery Util. Environ. Eff.* **2014**, *36*, 2009–2017. [CrossRef]
16. Dang, J.; Chou, K.-C. A Model for the Reduction of Metal Oxides by Carbon Monoxide. *ISIJ Int.* **2018**, *58*, 585–593. [CrossRef]
17. Jiang, Y.; Zong, P.; Tian, B.; Xu, F.; Tian, Y.; Qiao, Y.; Zhang, J. Pyrolysis behaviors and product distribution of Shenmu coal at high heating rate: A study using TG-FTIR and Py-GC/MS. *Energy Convers. Manag.* **2019**, *179*, 72–80. [CrossRef]
18. Czajka, K.M.; Modliński, N.; Kisiela-Czajka, A.M.; Naidoo, R.; Peta, S.; Nyangwa, B. Volatile matter release from coal at different heating rates–experimental study and kinetic modelling. *J. Anal. Appl. Pyrolysis* **2019**, *139*, 282–290. [CrossRef]
19. Vyazovkin, S.; Burnham, A.K.; Criado, J.M.; Pérez-Maqueda, L.A.; Popescu, C.; Sbirrazzuoli, N. ICTAC Kinetics Committee recommendations for performing kinetic computations on thermal analysis data. *Thermochim. Acta* **2011**, *520*, 1–19. [CrossRef]
20. Hammam, A.; Li, Y.; Nie, H.; Zan, L.; Ding, W.; Ge, Y.; Li, M.; Omran, M.; Yu, Y. Isothermal and Non-Isothermal Reduction Behaviors of Iron Ore Compacts in Pure Hydrogen Atmosphere and Kinetic Analysis. *Min. Metall. Explor.* **2020**, *38*, 81–93. [CrossRef]
21. Cai, J.; Wu, W.; Liu, R.; Huber, G.W. A distributed activation energy model for the pyrolysis of lignocellulosic biomass. *Green Chem.* **2013**, *15*, 1331–1340. [CrossRef]
22. Shen, D.K.; Gu, S.; Jin, B.; Fang, M.X. Thermal degradation mechanisms of wood under inert and oxidative environments using DAEM methods. *Bioresour. Technol.* **2011**, *102*, 2047–2052. [CrossRef]
23. Tian, B.; Qiao, Y.Y.; Tian, Y.Y.; Liu, Q. Investigation on the effect of particle size and heating rate on pyrolysis characteristics of a bituminous coal by TG–FTIR. *J. Anal. Appl. Pyrolysis* **2016**, *121*, 376–386. [CrossRef]
24. Zhao, H.; Li, Y.; Song, Q.; Lv, J.; Shu, Y.; Liang, X.; Shu, X. Effects of Iron Ores on the Pyrolysis Characteristics of a Low-Rank Bituminous Coal. *Energy Fuels* **2016**, *30*, 3831–3839. [CrossRef]
25. Wang, M.; Li, Z.; Huang, W.; Yang, J.; Xue, H. Coal pyrolysis characteristics by TG–MS and its late gas generation potential. *Fuel* **2015**, *156*, 243–253. [CrossRef]